Synchronized source of indistinguishable photons for quantum networks

NIJIL LAL,[1,*] IVAN A. BURENKOV,[1,2] YA-SHIAN LI-BABOUD,[1] M. V. JABIR [1], PAULINA S. KUO,[1] THOMAS GERRITS,[1] OLIVER SLATTERY,[1] AND SERGEY V. POLYAKOV[1,3]

[1]*National Institute of Standards and Technology, 100 Bureau Dr., Gaithersburg, MD 20899, USA*
[2]*Joint Quantum Institute & University of Maryland, College Park, MD 20742, USA*
[3]*Department of Physics, University of Maryland, College Park, MD 20742, USA*
[*]*nijillalck@gmail.com*

Abstract: We present a source of indistinguishable photons at telecom wavelength, synchronized to an external clock, for the use in distributed quantum networks. We characterize the indistinguishability of photons generated in independent parametric down-conversion events using a Hong-Ou-Mandel interferometer, and show non-classical interference with coalescence, C = 0.83(5). We also demonstrate the synchronization to an external clock within sub-picosecond timing jitter, which is significantly shorter than the single-photon wavepacket duration of ≈ 35 ps. Our source enables scalable quantum protocols over multi-node, long-distance optical networks using network-based clock recovery systems.

1. Introduction

Offering fast, efficient, and decoherence-free quantum information transfer, photonic qubits are widely acknowledged as the most desirable carriers for quantum communication [1]. Particularly, photonics enables the development of large-scale local and metropolitan quantum networks [2--5]. Scaling laboratory-level prototype quantum communication networks to real-world modular networks comes with a set of new, fundamental requirements on the components. For instance, single-photon sources must produce highly indistinguishable photons for such network use, because most network protocols require quantum interference of photons originating from independent sources. Examples of those protocols include teleportation and entanglement swapping [6--8]. Recent studies have achieved sources with very high indistinguishability [9--11], however a successful realization of synchronization of such sources to a network comaptible clock recovery system is missing so far. To create a network synchronized source, we need a pulsed pump laser that can be synchronized with an external network clock. It turns out that synchronizing the clocks at the distant network nodes, such that a typical single-mode single-photon source can be used, cannot be done at present. To achieve this, the source should be able to produce single-photon pulses with their pulse duration longer than the timing mismatch between the synchronized network clocks, which presently amounts to ∼ 1 ps [12]. In this work, we present such a source of indistinguishable photons in the telecommunication band with sub-picosecond pulse emission synchronization.

The indistinguishability of single photons depends on various factors such as their polarization, arrival time, spatial and temporal modes etc. Their spatial single-mode character could be guaranteed by using single-mode telecom fiber to couple the photons. The polarization could be stabilized using active polarization control interspersed with communication signals. The carrier frequency can be locally stabilized. Time of arrival of the interfering photon pulses could be adjusted as the relative path difference. In addition to these, single temporal mode or (Fourier) transform-limited pulse shape [13] is crucial for the quantum interference between independent photons. Both probabilistic [14, 15] and deterministic [16--18] single-photon sources (SPSs) have been extensively studied in the past to generate indistinguishable photons. Recently some preliminary measurements were made on the indistinguishability of photons from a single quantum

dot (QD) [19, 20] and two independent QDs [21] in the C-band. While such deterministic single-photon sources theoretically can achieve 100% efficiency, currently, their indistinguishability performance is significantly limited, unless post-selected, conditioned on nearly-simultaneous coincidence detection. The effects of dephasing and spectral diffusion [22, 23] also limit the realization of scalable QD-based network sources in the C-band, which may be improved in the future similarly to [24]. On the other hand, spontaneous parametric down-conversion (SPDC) allows convenient generation of indistinguishable photons in the telecom C-band and room temperature operation and, therefore, comes with significantly simplified experimental overhead which enables to build and operate network-separated indistinguishable sources.

As it pertains to heralded single photons from SPDC, their spatiotemporal properties are derived from both the spatiotemporal properties of the pump laser and the phase-matching curve of the SPDC crystal [11, 25]. Due to the nature of the parametric down-conversion that results in multi-mode output, additional spectral filtering may be required to achieve a transform-limited pulse shape for the generated photons. In addition, when more than one source is used in a network, the emission of photons from these sources should be synchronized, and such synchronization should be network-compatible. Quantum networks require the synchronization jitter ($\sim$ ps) to be significantly lower than what is typically available for commercial classical networks ($\sim$ sub-μs) and this represents a significant additional challenge.

To meet all the above requirements, we designed a source that can readily produce photons for multi-node quantum networks. Particularly, the source features $\approx$ 35 ps full width at half maximum (FWHM) heralded single-photon pulses with the spectral bandwidth of 0.1 nm and a carrier wavelength of 1550 nm. We measure a high degree of indistinguishability, characterized by a coalescence of 0.83(5). We demonstrate synchronization for practical network clock recovery methods and measure sub-ps short-term jitter as well as long-term time deviation below 10 ps. We find that the long-term time deviation is limited by the properties of clock recovery systems.

2. Source design

Quantum network protocols require indistinguishable (single-mode, Fourier transform-limited) single photons with their pulse duration longer than the timing mismatch achievable between the network nodes. The main challenge of building network compatible SPS is that the pulses produced by such sources are limited in pulse duration to a very narrow range. The photon pulse duration for a network source is mainly limited by two factors. First, it should be significantly longer than the expected jitter in the external clock signal. Secondly, longer pulses require progressively narrower bandwidths to be transform-limited, which is constrained by the length of the periodically poled nonlinear crystal or by the bandwidth of a spectral filter if one is used. Since long picosecond-scale, Fourier transform-limited single photon pulses cannot be generated by SPDC crystals, because the crystals cannot be made sufficiently long (150 mm or longer), these photons should be spectrally filtered. Ultra-narrow filters require active stabilization, which would complicate their field use. Thus, practical sub-nanometer filters set the upper bound on photon pulse duration. However, the use of a filter reduces the single-photon emission rate, which is undesirable. In addition to using a spectrally-efficient SPDC crystal, one requires a transform-limited or nearly-transform-limited pump laser with a pulse duration that matches the desired duration of single photons, because SPDC efficiency depends on the pump spectral bandwidth. Most picosecond pump lasers that can be externally synchronized are significantly multimode and this poses an additional challenge in building a network source of single-mode single photons. Also, the pump laser has to be synchronized to the network clock without adding any extra jitter. Prior research shows that the jitter associated with the White Rabbit (WR) [26] Precision Time Protocol (WR-PTP), which has now been standardized as part of the high-accuracy precision time protocol (HA-PTP) [27], can be made as low as a

few picoseconds [12] and hence could be an appropriate network-compatible clock. This jitter necessitates a source of single photons that are *longer* than ≈ 10 ps. On the other hand, to avoid active stabilization, the photons should be ≈ 0.1 nm or broader, which necessitates the pulse duration of ≈ 35 ps (Gaussian FWHM) or *shorter*. Taken together, these considerations decisively place single-photon pulse duration in the range of 10 ps - 35 ps.

To match these conditions, and to build the source with maximal possible efficiency, we chose a 30 mm quasi-phase-matched periodically poled $KTiOPO_4$ (PPKTP) crystal (poling period 46.15 microns, temperature at 40 °C) for collinear type-II photon pair generation with both signal and idler at 1550 nm (Fig. 1a). In addition, we use a volume Bragg grating (VBG) of 0.1 nm

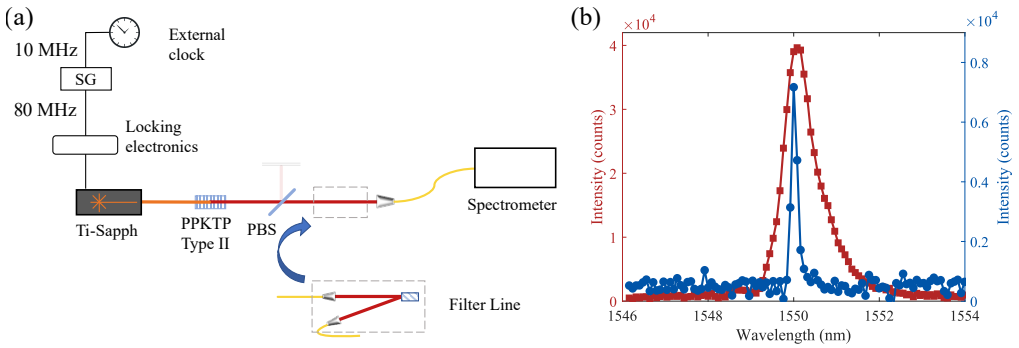

Fig. 1. Source design. (a) A low jitter singal generator (SG) transforms 10 MHz signal from the external clock to an 80 MHz sinusoidal signal that feeds the locking electronics associated with the Ti-Sapphire pump laser. One photon from the parametric down-converted pair goes through volume Bragg grating (VBG) which thereby optically filter the heralded single-photon output to ensure single-mode operation. (b) the spectrum of SPDC photons (red squares) and filtered signal photons with VBG in place (blue circles).

bandwidth to filter heralded single photons to nearly single time-bandwidth mode, which yields indistinguishable photons of ≈ 35 ps pulse duration. We use as a pump, a pulsed Ti:Sapphire laser that generates ≈ 10 ps nearly transform-limited pulses synchronously to an external clock. The pump laser (Spectra-Physics Tsunami [26]) is equipped with off-the-shelf locking capability that can actively stabilize the cavity length to synchronize the laser pulses to the external clock signal. Therefore, the laser can follow the network clock synchronization signal, which is the goal for multiple network nodes in a network. The 10 MHz signal from the external clock is transformed to an 80 MHz sinusoidal signal, that feeds the locking electronics associated with the Ti-Sapphire laser using a low-jitter signal generator.

To verify the bandwidth of the source, we measure the spectrum of signal photons directly after the crystal as well as through the grating filter (Fig. 1b). The spectrum of the unfiltered signal (idler) photon yields an estimated bandwidth of 0.88 nm (FWHM). Note that the large bandwidth of the unfiltered source is due to the crystal's length. Because the longest available crystals were used, the use of the filter is unavoidable for a single-mode operation. The spectral width (FWHM) of the filtered photon was measured to be 0.16 nm. It should be noted that these measurements are limited by the 0.08 nm resolution of the spectrometer used for the measurements. This result is in agreement with the nominal pass-band of the VBG (0.1 nm). Given the pass-band and assuming transform-limited photons with Gaussian pulse shape, the pulse duration of filtered single photons is 35.3 ps. To compare, if our source matched the laser pulse duration of 10 ps, the bandwidth for transform-limited operation would have been 0.353 nm. The source emission rate after spectral filtering is 10^3 counts/s/mW with a coincidence-to-accidental ratio of ~ 150. As expected, spectral filtering results in a reduction in count rate by approximately an order of

magnitude.

3. Synchronization to external clocks

3.1. Local synchronization

The successful synchronization of the source to an external clock is the first step in building a scalable network source of single photons. We demonstrate robust synchronization of our source to (1) the 10 MHz clock signal from a rubidium (Rb) atomic clock frequency standard and (2) the same clock distributed over a laboratory-scale network and recovered by a WR-PTP switch. A fast photodiode is used to measure the output of the laser and the time tag for each laser pulse

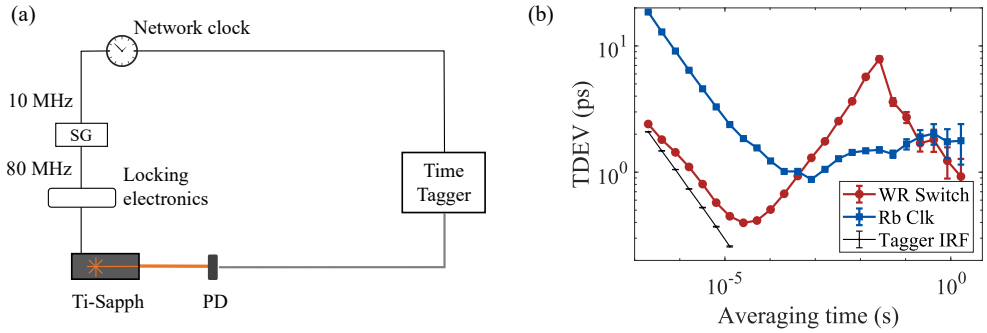

Fig. 2. (a) Experimental schematic for the synchronization of the pump laser pulses with a network clock. The pump laser pulses are detected with a fast photodiode (PD, 2 GHz bandwith). (b) Time deviation (TDEV) of the timing jitter in the laser when synchronized to the network clock from a low-jitter WR switch (red circles) and a Rb clock (blue squares). The combination of the two observations provide evidence of sub-picosecond jitter at short averaging times, and below 2 ps deviations at longer averaging times for our source ability to follow the external clock. See text for details. The black curve in (b) corresponds to the time tagger instrument response function (IRF), a baseline of our measurement.

is registered using low jitter time tagging electronics whose intrinsic jitter is ≈ 2 ps (Figure 2a). The measured time deviation (TDEV) gives a statistical measure of frequency fluctuations and hence provides information about the stability of the laser synchronization to an external clock. Figure 2b shows the TDEV of the synchronized laser output relative to the 10 MHz signal from the external Rb clock as well as the clock distributed by a WR switch.

It is worth noting that on a short timescale, for the measurements with the WR-distributed clock, the measured TDEV is limited by the intrinsic jitter of the time tagging electronics. Noise features around the millisecond-region are common to the WR recovery systems, and most likely attributed to the phase noise present in the Gigabit transceivers and phase detectors [12, 28]. To independently test the performance of the synchronization in this region, we have used the Rb clock as a direct input for synchronization. In this case, an improved stability of < 2 ps TDEV is observed for longer averaging times (Fig. 2b). However, the measured jitter is significantly higher at a short time scale. This excess jitter is not surprising, because the output signal from the commercial frequency standard is sinusoidal, which is slow rising compared to rectangular signals and can result in increased short-term jitter. The sine wave output could be converted to other forms (e.g., rectangular), but such a conversion is not trivial, because it could introduce jitter (due to edge detection, as seen in our work) or could lead to longer-term drift (due to an added disciplined local oscillator). The WRPTP system is essentially doing the latter by converting the 10 MHz sine clock from the frequency standard to 10 MHz rectangular pulses. Here we have

used the Rb-clock output, that was otherwise acting as the input for the WR system, as is to verify that the drift that is observed on a millisecond time scale (Fig. 2b) is originating from the WR electronics. Altogether, the synchronization analysis provides the evidence of a source of single photons that follows the external clock with sub-picosecond jitter and picosecond-level longer-term deviations. Note that there is an independent way to estimate jitter by a quantum measurement which we describe in section 4.

3.2. Network synchronization

Network clock synchronization over fiber is crucial for implementing quantum networking protocols. Here we verify the timing stability of the synchronization of two network clocks, a WR

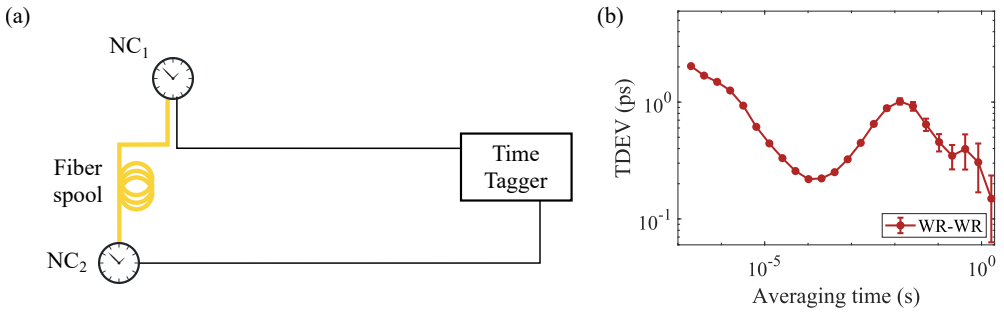

Fig. 3. (a) Experimental setup for measuring the timing stability in the synchronization between two network clocks (NC_1 & NC_2). (b) Time deviation (TDEV) analysis of the timing jitter in the synchronization of two network clocks, a WR timeTransmitter and a WR timeReceiver. The two white rabbit switches are separated by 88 km fiber.

timeTransmitter and a WR timeReceiver, separated by an 88 km fiber spool. The TDEV for the timing jitter associated with the synchronization of these two distributed network clocks is plotted in Fig. 3. Similar to the observations in the case of local synchronization, the jitter is an order of magnitude smaller when compared to the pulse duration of the network-compatible single-photon source under study. The TDEV analysis shows good timing stability at larger averaging times, demonstrating the synchronization between two telecommunications network-compatible optical two-way time transfer methods.

4. Two photon interference and indistinguishability

We study the interference of two pump-synchronized transform-limited heralded single photons that originate from different pump pulses. The twin photons generated in the Type-II SPDC process are separated using a polarizing beamsplitter (Fig. 4). Heralding (idler) photons are detected directly and used to herald the photon in the signal field. The heralded (signal) photons, after spectral filtering, pass through a non-polarizing fiber beamsplitter and are then sent to a Hong-Ou-Mandel (HOM) [29] interferometer through fiber patches of unequal length. The indistinguishability is measured as the lack of coincident photon detections between the two output ports of the HOM interferometer [23, 30], which can also be quantified as the interference visibility or coalescence (Entry 2.5.4 in Ref. [31]). For ideal indistinguishable photons arriving at the HOM beam splitter with perfect overlap, coalescence is perfect (defined as unity). For fully distinguishable photons the coalescence is zero. Each photon may arrive at the final beamsplitter in the HOM interferometer (FBS_2) through a short path or a long path. The optical delay between the short and long paths in the interferometer is adjusted (using the adjustable free-space "trombone" delay line and adding necessary fiber lengths) such that both photons temporally overlap at FBS_2. Specifically, to observe the interference between heralded single

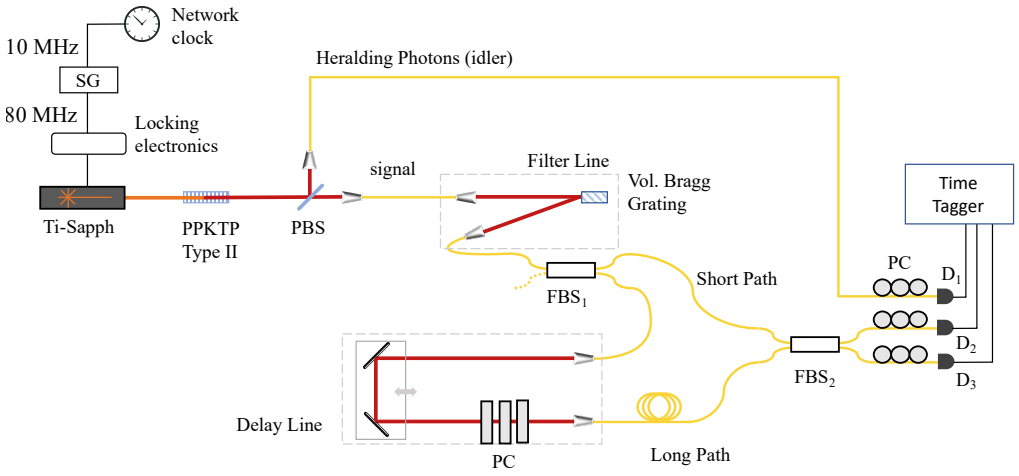

Fig. 4. The experimental schematic for the interference between indistinguishable photons generated in independent events from the same source. The idler photon is used for heralding while the signal photon undergoes spectral filtering and then enters the interferometer. PBS - polarizing beam splitter, PC - polarization controller, FBS - nonpolarizing fiber beam splitter, D - single-photon detector.

photons that are generated n-pulses apart, the delay between the short path and long path, t_n, is set such that an "early" photon (associated with pulse #1), that happened to take the long path arrives simultaneously with a "late" photon (associated with pulse #n, n > 1) that took the short path (Fig. 5a). If the photons are indistinguishable, they coalesce at the final beamsplitter (FBS_2) via quantum interference [22], conditioned upon the detection of both the heralding photons (H_1 and H_n) in the idler arm.

To measure this double-heralded second order correlation, we use the protocol illustrated in Fig. 5. When a heralding photon is registered in the idler detector, we look for a second herald in the same detector corresponding to the "late" signal photon. In our experiment, the path difference between the short path and long path of the interferometer is maintained as 9 times the pulse separation. Once this double-heralding is successful, we look for coincident signal photon detection between the two output detectors of the interferometer. Each signal photon in a double-heralded coincidence detection belong to an "early" pulse or a "late" pulse. The indistinguishability of these independent signal photons will result in reduced double-heralded coincidences and subsequently be manifested as the HOM dip. Coincidences may arise when distinguishable photons arrive simultaneously (one through short path and the other through long path), as shown in Fig. 5a. Because this source is probabilistic, heralded higher-order states are fundamentally present [32]. Thus, coincidences can also arise from heralded multiphoton states. In our source, two-photon states dominate the multiphoton output and the contribution from three- and higher-photon states can be neglected. Conditional (double-heralded) second-order correlations are calculated from four-fold coincidence detections, where detection times are registered using a time tagger. The experimentally obtained HOM dip is shown in Fig. 6a. The horizontal axis is the additional path delay (Δl) introduced with the optical trombone placed in the long arm of the interferometer. Figure 6b shows raw coincidences as a function of heralded trial number differences (Δ) (Entry 2.6.3 and 2.6.7 in Ref. [31]). In measuring double-heralded (D.-H.) events, 'Δ' corresponds to the probabilistic occurrence of the next double-heralded trial. In our case, a D.-H. trial occurs when two heralding photons are detected exactly 9 pulse periods (112.5 ns) apart. Here, Δ is the enumerative difference, i-j, where i and j represent two D.-H. events. Because all detection events are recorded, the identification of D.-H. trials can be done

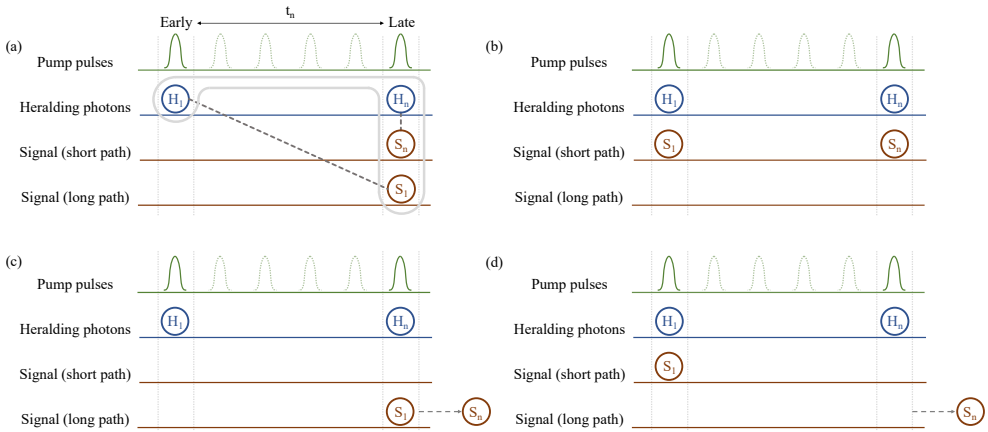

Fig. 5. Illustration of the protocol to measure indistinguishability of single photons via a double-heralded HOM interference. (a) Once two photons are detected in the heralding arm consecutively (H_1 & H_n) with a time separation t_n, coincidence counts are estimated between the output ports of the interferometer in the signal arm. HOM interference can happen only when an "early" signal photon (S_1) and a "late" signal photon (S_n) arrive near-simultaneously in the same bin, as shown in (a). All other outcomes (b, c and d) do not contribute to the doubly-heralded coincidence counts. However, if photons S_1 and S_n are indistinguishable, HOM interference will prevent coincidence detection.

in post-processing. $\Delta = 0$ corresponds to the D.-H. events where the photons simultaneously arrive at the beamsplitter FBS_2. Here, coincidences between detectors D_2 and D_3 give rise to the quantum interference peak seen in Fig. 6a. For $\Delta = 1$, we look for a detection on detector D_2 corresponding to the D.-H. trial, i, and a detection on detector D_3 corresponding to the D.-H. trial, i+1. For $\Delta = 2$, the D.-H. coincidences corresponding to trials i and i+2 are assessed and so on. Clearly, in these cases, photons detected by D_2 and D_3 do not meet on FBS_2. Here, the coincidences are random and are used for normalizing the HOM curve. Note that the larger histogram bins in Fig. 6b are separated as the difference in the conditional event number (Δ), and not a time delay. The shoulders of the dip saturate at 0.5 due to splitting the single-photon output into two arms [22, 33].

When the two independent single-photon pulses perfectly overlap on top of each other, we reach the minimum of the dip that reads 0.144 ± 0.014, corresponding to the raw coalescence, $C_{\text{raw}} = 0.712 \pm 0.028$. The value of the expected FWHM of the dip was calculated from the convolution of two identical photon pulses, assuming a Gaussian pulse shape. The convolution of two Gaussians results in a Gaussian, whose FWHM is $\sqrt{2}$ times wider than the FWHM of the individual pulses. For our transform-limited photons whose spectral bandwidth is 0.1 nm, the pulse duration is 35.3 ps. Hence, the resulting convolution should nominally correspond to $\sqrt{2}\times$35.3 ps, which translates to 15.1 mm optical path length in our trombone delay line. From our measurement, the dip FWHM turns out to be 15.3 mm. The difference between the estimated and measured FWHM of the HOM dip can be attributed to the timing jitter in the system (that modifies the individual photon pulse arrival times), and a back calculation provides the estimation of the jitter that is responsible for this difference, under this assumption, to be less than 1 ps (0.5 ps), in agreement with the synchronization study discussed in Section 3. However, this estimate is based on certain assumptions, such as the bandpass of the VBG filter of exactly 0.1 nm and the Gaussian photon pulse shape. Hence, we have given a more conservative estimate in the following discussion, that is obtained directly from the coalescence, C, and does not

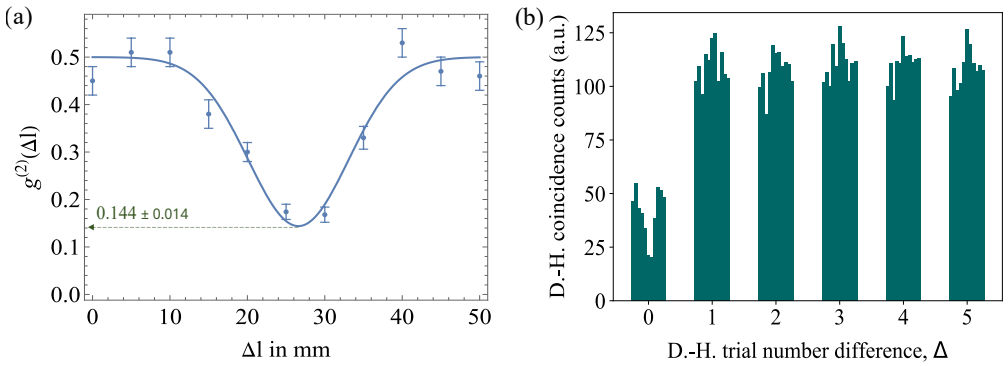

Fig. 6. (a) Normalized double-heralded second-order correlation function that shows HOM interference plotted as a function of the additional optical delay (Δl) between the short and long arms of the interferometer. (b) Raw coicidences that show correlation within the same double-heralded (D.-H.) trial (peak at Δ = 0) and between trials (other peaks). Quantum interference (given in (a)) occur only within the same trial (Δ = 0), whereas other cases (Δ > 0) yield statistical correlations and are used for normalization. Because the horizontal axis enumerates trial number differences when the condition is satisfied, delays between the peaks are random, and hence the horizontal axis does not represent a continuous time.

require any additional assumptions.

Because coincidences can occur due to multi-photon states in the single-photon channel of our setup, the coalescence C of single photons is higher (better) than the observed C_{raw}. Because higher-order multi-photon states occur very rarely, we consider the case with 0-, 1-, and 2-photon states for simplicity:

$$|\Psi\rangle_a = \sqrt{p_{0a}}\,|0\rangle + \sqrt{p_{1a}}\,|1\rangle + \sqrt{p_{2a}}\,|2\rangle \tag{1}$$

$$|\Psi\rangle_b = \sqrt{p_{0b}}\,|0\rangle + \sqrt{p_{1b}}\,|1\rangle + \sqrt{p_{2b}}\,|2\rangle \tag{2}$$

where $|\Psi\rangle_a(|\Psi\rangle_b)$ is the superposition state that impinge on the input port a(b) of the HOM beamsplitter (FBS_2 in Fig. 4) and $p_{ja(jb)}$ is the probability corresponding to each eigen state $|j\rangle$. In this approximation, the probability of a two-photon state to occur in port $a(b)$ is $p_{2a(2b)} = \frac{1}{2} g^{(2)}_{\text{HBT}a(b)}(0) p^2_{1a(1b)}$, where $g^{(2)}_{\text{HBT}a(b)}(0)$ is the second-order autocorrelation function in the $a(b)$ input of the interferometer. Therefore, the coalescence, C, correcting for the two-photon output of the source, can be derived from the equation,

$$\frac{G^2_{\text{HOM}}(\Delta\ell = 0)}{G^2_{\text{HOM}}(\Delta\ell > \ell_{\text{overlap}})} = \frac{p_{1a}p_{1b}(1-C) + \frac{1}{2}p_{0a}p^2_{1b}g^{(2)}_{\text{HBT}b}(0) + \frac{1}{2}p_{0b}p^2_{1a}g^{(2)}_{\text{HBT}a}(0)}{p_{1a}p_{1b} + \frac{1}{2}p_{0a}p^2_{1b}g^{(2)}_{\text{HBT}b}(0) + \frac{1}{2}p_{0b}p^2_{1a}g^{(2)}_{\text{HBT}a}(0)} \tag{3}$$

where $\Delta\ell$ is the relative path difference between interfering photon pulses and ℓ_{overlap} is the range of their convolution. To compute probabilities, we measure the second-order correlation in both arms of the HOM interferometer, using the Hanbury Brown-Twiss (HBT) measurement [34]. We find $g^{(2)}_{\text{HBT}a}(0) = 0.12 \pm 0.02$ and $g^{(2)}_{\text{HBT}b}(0) = 0.14 \pm 0.04$ for the short and long path of the interferometer respectively (measured by blocking the other arm in the interferometer). The HBT measurements in both arms agree to within the uncertainty and indicate that the beamsplitter is fair. The observed values of the second order coherence function, $g^{(2)}_{\text{HBT}}(0)$, corresponds to the operating pump power, 100 mW. While smaller values for $g^{(2)}_{\text{HBT}}(0)$ can be obtained for SPDC sources by maintaining lower pair generation rates, high rates are required for communication

over quantum networks to overcome losses in long fiber links. There are some established engineering techniques that can marginally enhance the single-photon purity and other source efficiency metrics [11, 35, 36]. However, these methods cannot be directly implemented for single-photon pulses longer than 1 ps.

The correction for two-photon events yields $C = 0.83 \pm 0.05$ for single photons emitted by the source. We conclude that the source generates single photons with high indistinguishability, which is the goal of this effort. We can now obtain the independent upper bound on jitter in the system, assuming that the coalescence reduction from unity is only due to single-photon source jitter. Attributing indistinguishability reduction to only jitter yields the upper bound that relies on the quantum measurement with no extra assumptions, and it is independent from other jitter estimations. Using the formula (given in Ref. [12]) that determines the indistinguishability (I) from the overlap of two Gaussian photon pulses of root mean square (RMS) width σ,

$$I = \frac{1}{\sqrt{1 + \frac{\delta t^2}{2\sigma^2}}} \tag{4}$$

where δt is the RMS width of the normal distribution describing the clock synchronization jitter, we estimate the upper bound on the jitter as $\tau \leq 10$ ps RMS. This is less than the pulse duration of interfering photons and in agreement with the TDEV measurements.

5. Conclusions

We have successfully created a source of indistinguishable photons in the telecom C-band that can be used for quantum networks. This source is synchronized to an external Rubidium clock, distributed using the White Rabbit precision time protocol with sub-picosecond short-term and picosecond-level long-term jitter. Our experiment verifies that the single-photon source meets several design constraints required for its practical use in quantum networks, including those needed for HOM interference of the photonic qubits: single spatial and temporal-bandwidth mode of operation, picosecond-level long term synchronization timing jitter, pulse duration of ≈ 35 ps that is compatible with the timing jitter, and high single-photon generation rate. The transform-limited pump pulses improve the efficiency of single-mode SPDC photon generation. In addition, our source can be pumped with very high optical power, limited only by possible crystal breakdown. This allows our source to achieve high photon generation rates, which is crucial for a quantum network source to overcome transmission losses through fiber. This paper describes characterization of the source and reports on meeting all design constraints, verified by classical and quantum measurements. Particularly, the desired time stability in synchronization of the source to an external network clock was confirmed by the time deviation (TDEV) analysis. Pulse duration was found from spectral and temporal measurements. We have also characterized the indistinguishability of the generated single photons via Hong-Ou-Mandel interferometry. This quantum measurement independently establishes high nonclassical coalescence, and confirms classical characterization of the photon wavepacket duration and single-photon source jitter. In summary, we present a source that is designed for a very particular key application in quantum networks, that is to provide network-synchronizable indistinguishable photons in the telecom C-band compatible with quantum protocols using HOM interference. This source can also be a possible platform for developing practical entangled pair sources for quantum networks. The commercial availability of this network source may serve as a scalable modular unit in a multi-node, long distance quantum network infrastructure.

Acknowledgements. The authors would like to express their gratitude to Dr. Daehyun Ahn for the fruitful discussion regarding quantum dot based sources.

Disclosures. The authors declare no conflicts of interest.

Data availability. Data underlying the results presented in this paper are not publicly available at this time but may be obtained from the authors upon reasonable request.

References

1. F. Flamini, N. Spagnolo, and F. Sciarrino, ''Photonic quantum information processing: a review,'' Reports on Prog. Phys. **82**, 016001 (2018).
2. M. Peev, C. Pacher, R. Alléaume, C. Barreiro, J. Bouda, W. Boxleitner, T. Debuisschert, E. Diamanti, M. Dianati, J. F. Dynes, S. Fasel, S. Fossier, M. Fürst, J.-D. Gautier, O. Gay, N. Gisin, P. Grangier, A. Happe, Y. Hasani, M. Hentschel, H. Hübel, G. Humer, T. Länger, M. Legré, R. Lieger, J. Lodewyck, T. Lorünser, N. Lütkenhaus, A. Marhold, T. Matyus, O. Maurhart, L. Monat, S. Nauerth, J.-B. Page, A. Poppe, E. Querasser, G. Ribordy, S. Robyr, L. Salvail, A. W. Sharpe, A. J. Shields, D. Stucki, M. Suda, C. Tamas, T. Themel, R. T. Thew, Y. Thoma, A. Treiber, P. Trinkler, R. Tualle-Brouri, F. Vannel, N. Walenta, H. Weier, H. Weinfurter, I. Wimberger, Z. L. Yuan, H. Zbinden, and A. Zeilinger, ''The secoqc quantum key distribution network in vienna,'' New J. Phys. **11**, 075001 (2009).
3. D. Stucki, M. Legré, F. Buntschu, B. Clausen, N. Felber, N. Gisin, L. Henzen, P. Junod, G. Litzistorf, P. Monbaron, L. Monat, J.-B. Page, D. Perroud, G. Ribordy, A. Rochas, S. Robyr, J. Tavares, R. Thew, P. Trinkler, S. Ventura, R. Voirol, N. Walenta, and H. Zbinden, ''Long-term performance of the swissquantum quantum key distribution network in a field environment,'' New J. Phys. **13**, 123001 (2011).
4. M. Sasaki, M. Fujiwara, H. Ishizuka, W. Klaus, K. Wakui, M. Takeoka, S. Miki, T. Yamashita, Z. Wang, A. Tanaka, K. Yoshino, Y. Nambu, S. Takahashi, A. Tajima, A. Tomita, T. Domeki, T. Hasegawa, Y. Sakai, H. Kobayashi, T. Asai, K. Shimizu, T. Tokura, T. Tsurumaru, M. Matsui, T. Honjo, K. Tamaki, H. Takesue, Y. Tokura, J. F. Dynes, A. R. Dixon, A. W. Sharpe, Z. L. Yuan, A. J. Shields, S. Uchikoga, M. Legré, S. Robyr, P. Trinkler, L. Monat, J.-B. Page, G. Ribordy, A. Poppe, A. Allacher, O. Maurhart, T. Länger, M. Peev, and A. Zeilinger, ''Field test of quantum key distribution in the tokyo qkd network,'' Opt. Express **19**, 10387--10409 (2011).
5. J. F. Dynes, A. Wonfor, W. W.-S. Tam, A. W. Sharpe, R. Takahashi, M. Lucamarini, A. Plews, Z. L. Yuan, A. R. Dixon, J. Cho, Y. Tanizawa, J.-P. Elbers, H. Greißer, I. H. White, R. V. Penty, and A. J. Shields, ''Cambridge quantum network,'' npj Quantum Inf. **5**, 101 (2019).
6. R.-B. Jin, M. Takeoka, U. Takagi, R. Shimizu, and M. Sasaki, ''Highly efficient entanglement swapping and teleportation at telecom wavelength,'' Sci. Reports **5**, 9333 (2015).
7. M. Pant, H. Krovi, D. Towsley, L. Tassiulas, L. Jiang, P. Basu, D. Englund, and S. Guha, ''Routing entanglement in the quantum internet,'' npj Quantum Inf. **5**, 25 (2019).
8. Y. Wang, Z.-Y. Hao, Z.-H. Liu, K. Sun, J.-S. Xu, C.-F. Li, G.-C. Guo, A. Castellini, B. Bellomo, G. Compagno, and R. Lo Franco, ''Remote entanglement distribution in a quantum network via multinode indistinguishability of photons,'' Phys. Rev. A **106**, 032609 (2022).
9. R.-B. Jin, K. Wakui, R. Shimizu, H. Benichi, S. Miki, T. Yamashita, H. Terai, Z. Wang, M. Fujiwara, and M. Sasaki, ''Nonclassical interference between independent intrinsically pure single photons at telecommunication wavelength,'' Phys. Rev. A **87**, 063801 (2013).
10. M. M. Weston, H. M. Chrzanowski, S. Wollmann, A. Boston, J. Ho, L. K. Shalm, V. B. Verma, M. S. Allman, S. W. Nam, R. B. Patel, S. Slussarenko, and G. J. Pryde, ''Efficient and pure femtosecond-pulse-length source of polarization-entangled photons,'' Opt. Express **24**, 10869--10879 (2016).
11. C. Chen, J. E. Heyes, K.-H. Hong, M. Y. Niu, A. E. Lita, T. Gerrits, S. W. Nam, J. H. Shapiro, and F. N. C. Wong, ''Indistinguishable single-mode photons from spectrally engineered biphotons,'' Opt. Express **27**, 11626--11634 (2019).
12. I. A. Burenkov, A. Semionov, Hala, T. Gerrits, A. Rahmouni, D. Anand, Y.-S. Li-Baboud, O. Slattery, A. Battou, and S. V. Polyakov, ''Synchronization and coexistence in quantum networks,'' Opt. Express **31**, 11431--11446 (2023).
13. F. W. Sun and C. W. Wong, ''Indistinguishability of independent single photons,'' Phys. Rev. A **79**, 013824 (2009).
14. A. B. U'Ren, Y. Jeronimo-Moreno, and H. Garcia-Gracia, ''Generation of fourier-transform-limited heralded single photons,'' Phys. Rev. A **75**, 023810 (2007).
15. B. Srivathsan, G. K. Gulati, B. Chng, G. Maslennikov, D. Matsukevich, and C. Kurtsiefer, ''Narrow band source of transform-limited photon pairs via four-wave mixing in a cold atomic ensemble,'' Phys. Rev. Lett. **111**, 123602 (2013).
16. L. Béguin, J.-P. Jahn, J. Wolters, M. Reindl, Y. Huo, R. Trotta, A. Rastelli, F. Ding, O. G. Schmidt, P. Treutlein, and R. J. Warburton, ''On-demand semiconductor source of 780-nm single photons with controlled temporal wave packets,'' Phys. Rev. B **97**, 205304 (2018).
17. A. V. Kuhlmann, J. H. Prechtel, J. Houel, A. Ludwig, D. Reuter, A. D. Wieck, and R. J. Warburton, ''Transform-limited single photons from a single quantum dot,'' Nat. Commun. **6**, 8204 (2015).
18. M. E. Trusheim, B. Pingault, N. H. Wan, M. Gündoğan, L. De Santis, R. Debroux, D. Gangloff, C. Purser, K. C. Chen, M. Walsh, J. J. Rose, J. N. Becker, B. Lienhard, E. Bersin, I. Paradeisanos, G. Wang, D. Lyzwa, A. R.-P. Montblanch, G. Malladi, H. Bakhru, A. C. Ferrari, I. A. Walmsley, M. Atatüre, and D. Englund, ''Transform-limited photons from a coherent tin-vacancy spin in diamond,'' Phys. Rev. Lett. **124**, 023602 (2020).
19. C. Nawrath, F. Olbrich, M. Paul, S. L. Portalupi, M. Jetter, and P. Michler, ''Coherence and indistinguishability of highly pure single photons from non-resonantly and resonantly excited telecom C-band quantum dots,'' Appl. Phys. Lett. **115**, 023103 (2019).

20. D. A. Vajner, P. Holewa, E. Zięba-Ostój, M. Wasiluk, M. von Helversen, A. Sakanas, A. Huck, K. Yvind, N. Gregersen, A. Musiał, M. Syperek, E. Semenova, and T. Heindel, ''On-demand generation of indistinguishable photons in the telecom c-band using quantum dot devices,'' ACS Photonics **11**, 339--347 (2024).
21. P. Holewa, E. Zięba-Ostój, D. A. Vajner, M. Wasiluk, B. Gaál, A. Sakanas, M. Burakowski, P. Mrowiński, B. Krajnik, M. Xiong, A. Huck, K. Yvind, N. Gregersen, A. Musiał, T. Heindel, M. Syperek, and E. Semenova, ''Scalable quantum photonic devices emitting indistinguishable photons in the telecom c-band,'' arXiv preprint arXiv:2304.02515 (2023).
22. E. B. Flagg, S. V. Polyakov, T. Thomay, and G. S. Solomon, ''Dynamics of nonclassical light from a single solid-state quantum emitter,'' Phys. Rev. Lett. **109**, 163601 (2012).
23. S. V. Polyakov, A. Muller, E. B. Flagg, A. Ling, N. Borjemscaia, E. Van Keuren, A. Migdall, and G. S. Solomon, ''Coalescence of single photons emitted by disparate single-photon sources: The example of inas quantum dots and parametric down-conversion sources,'' Phys. Rev. Lett. **107**, 157402 (2011).
24. J. C. Loredo, N. A. Zakaria, N. Somaschi, C. Anton, L. de Santis, V. Giesz, T. Grange, M. A. Broome, O. Gazzano, G. Coppola, I. Sagnes, A. Lemaitre, A. Auffeves, P. Senellart, M. P. Almeida, and A. G. White, ''Scalable performance in solid-state single-photon sources,'' Optica **3**, 433--440 (2016).
25. Z. Y. Ou, ''Parametric down-conversion with coherent pulse pumping and quantum interference between independent fields,'' Quantum Semiclassical Opt. J. Eur. Opt. Soc. Part B **9**, 599 (1997).
26. Commercial equipment and software referred to in this work is identified for informational purposes only, and does not imply recommendation of or endorsement by the National Institute of Standards and Technology, nor does it imply that the products so identified are necessarily the best available for the purpose.
27. ''IEEE standard for a precision clock synchronization protocol for networked measurement and control systems,'' IEEE Std 1588-2019 (Revision IEEE Std 1588-2008) pp. 1--499 (2020).
28. M. Rizzi, M. Lipinski, P. Ferrari, S. Rinaldi, and A. Flammini, ''White rabbit clock synchronization: Ultimate limits on close-in phase noise and short-term stability due to fpga implementation,'' IEEE Trans. on Ultrason. Ferroelectr. Freq. Control. **65**, 1726--1737 (2018).
29. C. K. Hong, Z. Y. Ou, and L. Mandel, ''Measurement of subpicosecond time intervals between two photons by interference,'' Phys. Rev. Lett. **59**, 2044--2046 (1987).
30. E. B. Flagg, A. Muller, S. V. Polyakov, A. Ling, A. Migdall, and G. S. Solomon, ''Interference of single photons from two separate semiconductor quantum dots,'' Phys. Rev. Lett. **104**, 137401 (2010).
31. J. C. Bienfang, T. Gerrits, P. S. Kuo, A. Migdall, S. Polyakov, and O. Slattery, ''Single-photon sources and detectors dictionary,'' (2023). (National Institute of Standards and Technology, Gaithersburg, MD), NIST IR 8486.
32. A. Migdall, S. V. Polyakov, J. Fan, and J. C. Bienfang, *Single-photon generation and detection: physics and applications* (Academic Press, 2013).
33. T. Thomay, S. V. Polyakov, O. Gazzano, E. Goldschmidt, Z. D. Eldredge, T. Huber, V. Loo, and G. S. Solomon, ''Simultaneous, full characterization of a single-photon state,'' Phys. Rev. X **7**, 041036 (2017).
34. R. H. Brown and R. Q. Twiss, ''Correlation between photons in two coherent beams of light,'' Nature **177**, 27--29 (1956).
35. L. K. Shalm, E. Meyer-Scott, B. G. Christensen, P. Bierhorst, M. A. Wayne, M. J. Stevens, T. Gerrits, S. Glancy, D. R. Hamel, M. S. Allman, K. J. Coakley, S. D. Dyer, C. Hodge, A. E. Lita, V. B. Verma, C. Lambrocco, E. Tortorici, A. L. Migdall, Y. Zhang, D. R. Kumor, W. H. Farr, F. Marsili, M. D. Shaw, J. A. Stern, C. Abellán, W. Amaya, V. Pruneri, T. Jennewein, M. W. Mitchell, P. G. Kwiat, J. C. Bienfang, R. P. Mirin, E. Knill, and S. W. Nam, ''Strong loophole-free test of local realism,'' Phys. Rev. Lett. **115**, 250402 (2015).
36. P. B. Dixon, J. H. Shapiro, and F. N. C. Wong, ''Spectral engineering by gaussian phase-matching for quantum photonics,'' Opt. Express **21**, 5879--5890 (2013).